



HAL
open science

One-flow feed divided electrochemical reactor for indirect electrolytic production of hypochlorite from brine for swimming pool treatment-experimental and theoretical optimization

Théodore Tzedakis, Yves Assouan

► **To cite this version:**

Théodore Tzedakis, Yves Assouan. One-flow feed divided electrochemical reactor for indirect electrolytic production of hypochlorite from brine for swimming pool treatment-experimental and theoretical optimization. *Chemical Engineering Journal*, 2014, 253, pp.427-437. 10.1016/j.cej.2014.05.001 . hal-01890148

HAL Id: hal-01890148

<https://hal.science/hal-01890148>

Submitted on 8 Oct 2018

HAL is a multi-disciplinary open access archive for the deposit and dissemination of scientific research documents, whether they are published or not. The documents may come from teaching and research institutions in France or abroad, or from public or private research centers.

L'archive ouverte pluridisciplinaire **HAL**, est destinée au dépôt et à la diffusion de documents scientifiques de niveau recherche, publiés ou non, émanant des établissements d'enseignement et de recherche français ou étrangers, des laboratoires publics ou privés.



Open Archive Toulouse Archive Ouverte

OATAO is an open access repository that collects the work of Toulouse researchers and makes it freely available over the web where possible

This is an author's version published in: <http://oatao.univ-toulouse.fr/20244>

Official URL: <https://dx.doi.org/10.1016/j.cej.2014.05.001>

To cite this version:

Tzedakis, Théodore  and Assouan, Yves  *One-flow feed divided electrochemical reactor for indirect electrolytic production of hypochlorite from brine for swimming pool treatment-experimental and theoretical optimization.* (2014) *Chemical Engineering Journal*, 253. 427-437. ISSN 1385-8947

Any correspondence concerning this service should be sent to the repository administrator: tech-oatao@listes-diff.inp-toulouse.fr

One-flow feed divided electrochemical reactor for indirect electrolytic production of hypochlorite from brine for swimming pool treatment-experimental and theoretical optimization

T. Tzedakis*, Y. Assouan

Laboratoire de Génie Chimique, Université de Toulouse – Paul Sabatier, 118, route de Narbonne, 31062 Toulouse, France

H I G H L I G H T S

- Optimization of an electrochemical chlorinator for swimming pool.
- Divided asymmetric electrochemical continuously stirred reactor.
- Convective transfer of the anolyte across the separator to the cathodic compartment.
- The brine (5 M NaCl) conversion reaches 50% under 3 kA m^{-2} with a faradic yield of 80%.
- Correlation of current density versus chloride concentration for concentrated brine.

A B S T R A C T

A 'two-compartment' asymmetric electrochemical reactor, operating without electrodes polarity inversion, was designed and optimized for the chlorination of swimming pools. Gaseous chlorine, produced at the anode and absorbed in the alkalized catholyte, provides the hypochlorite solution. Empiric equations providing the chloride concentration dependence on the initial current density magnitude were established. Experimental optimization of the effect of the various operating parameters allows a chloride conversion close to 50% with faradic yields higher than 80%, and a chlorine production of 1 kmol/day/m^2 to be achieved. Macroscopic mass balance, was performed and the obtained theoretical results correlate with the experimental ones ($X_{\text{theor.Cl}^-} - X_{\text{exper.Cl}^-} < 10\%$).

1. Introduction

Gaseous chlorine was produced at industrial scale by electrolysis of concentrated brine solution. Several studies focus on the production of chlorine, involving new material or processes, that enable saving electrical energy; thus the field is important to industrial production [1–7]. Furthermore, several commercial devices (chlorinators) exist that produce chlorine or hypochlorite, used for treating swimming pool water. Diluted brine solutions ($\text{NaCl} < 30 \text{ g L}^{-1}$), were electrolyzed using an undivided mono/bi polar electrochemical reactor, continuously supplied by swimming pool water.

DSA $\text{Ti/TiO}_2/\text{RuO}_2$, is the anodic material used for chloride oxidation to chlorine [8–10]. Titanium (or stainless steel) was used as the cathodic material.

Due to the neutral pH of the electrolyte, chloride oxidation directly produces hypochlorite (Table 1, R1) used in swimming pools. In fact, gaseous chlorine produced by electrolysis is transformed into hypochlorite following the disproportionation reaction (11 or 12, Table 1) by the action of soda [11,12]. Note that concentrated (50%) hypochlorite solutions were also produced by action of gaseous chlorine and soda.

Chlorinators can operate as a function of the geographical area for long periods; the main problem of these systems was due to the limescale which can deposit on the electrodes, mainly the Ti or steel cathodes (because of alkalization of the interface); indeed, during electrolyses the limescale cumulates on the electrode surface leading to short circuits and damage to the electrodes, so the system becomes inoperative.

Several devices have been patented in order to overcome the limescale deposit growth [12–14]. For automated chlorinators, one possibility consists of alternating the polarity of the electrodes [14]. A slight acidification of the interface of the cathode during the short anodic polarization causes dissolution of the limescale

Table 1
Various possible reactions during electrolysis of a brine solution (1–12) depending on the operating conditions (pH, T°C, [Cl⁻],...). The reaction (13) corresponds to the hypochlorite potentiometric titration.

Electrode	Main/acidic media pH < 3	N°	Side/neutral or slightly acidic media pH > 5	N°
Anode	Cl ⁻ → 1/2 Cl ₂ + e ⁻	(1)	Cl ⁻ + 2OH ⁻ → ClO ⁻ + 2e ⁻	(2)
	H ₂ O → 1/2 O ₂ + 2e ⁻ + 2H ⁺	(3)	OH ⁻ → 1/4 O ₂ + e ⁻ + 1/2 H ₂ O	(4)
	H ⁺ + e ⁻ → 1/2 H ₂	(5)	H ₂ O + e ⁻ → 1/2 H ₂ + OH ⁻	(6)
Cathode	ClO ⁻ + 2e ⁻ + 2H ⁺ → Cl ⁻ + H ₂ O	(7)	ClO ⁻ + 2e ⁻ + H ₂ O → Cl ⁻ + 2OH ⁻	(8)
	O ₂ + 4H ⁺ + 4e ⁻ → 2H ₂ O	(9)	O ₂ + 4e ⁻ + 2H ₂ O → 4OH ⁻	(10)
Cl ₂ disproportionation	(pH ~ ≥ 4) Cl ₂ + H ₂ O → HClO + Cl ⁻ + H ⁺	(11)	(pH ~ ≥ 7) Cl ₂ + 2OH ⁻ → ClO ⁻ + Cl ⁻ + H ₂ O	(12)
Hypochlorite titration	ClO ⁻ + SO ₃ ²⁻ → SO ₄ ²⁻ + Cl ⁻	(13)		

deposit enabling activation of the electrode. Even if this system appears efficient, after several 'electrodes polarity' inversions, the catalytic layer (Ru/Ti oxides) is damaged; hypochlorite production then drastically decreases and requires the electrodes to be changed.

The goals of this study are to design and optimize an electrochemical reactor dedicated to supplying active chlorine/hypochlorite for swimming pool. The main criteria that govern the design of this device are indicated below:

- it must operate without polarity inversion (to avoid destruction of the catalytic coating) to maximize the duration of the electrode material.
- as with the existing devices, the new proposed reactor has to operate automatically for the required duration (3–4 months), implying that it is supplied by a concentrated brine (sodium chloride ~300 g L⁻¹; ~5 mol L⁻¹), reducing the volume used.

To reach this goal, this study aims to design and optimize a divided electrochemical cell, continuously supplied in the anodic compartment by brine in slightly acidified (pH < 3), demineralized water. The electrolytic compartments are separated by a porous ceramic diaphragm allowing convective transfer of the anolyte to the cathodic compartment. Acidification of brine allows gaseous chlorine production; simultaneously, water (or H⁺) reduction to H₂ leads to alkalization of the catholyte and the production of soda. Absorption of gaseous chlorine in the catholyte (in the outlet of the cathodic compartment) leads to the production of hypochlorite.

Experimental and theoretical optimization of the various operating parameters (applied current density, electrolyte flow, pH adjustment of the solutions,...) for chloride conversion and chlorine converted to hypochlorite production, constitutes the main points involved below.

2. Experimental section: chemicals-analytical procedure and devices

Deionised water was used for all solutions. Chemicals were supplied by WVR. A divided electrochemical cell of a volume of 50 cm³ per compartment, was used to carry out the electrochemical kinetics studies. The electrolytic compartments were separated by a ceramic diaphragm of porosity 5. Current potential curves were plotted using a Potentiostat–Galvanostat (PGZ 100-Voltalab of Radiometer Analytical, and a VoltaMaster 4 software). The working electrode used was a chlorine/DSA[®] plate (24 mm²) e.g. titanium grids covered by a catalytic layer of metallic oxides from Ru/Ti/In-DSA[®] from ELTECH. A platinum rod was used as auxiliary electrode and the reference electrode was a silver/silver chloride (Ag/AgCl/KCl saturated).

Divided electrochemical cells with volume ratio ($V_{\text{anolyte}}/V_{\text{catholyte}} \sim 2$) were used to carry out preparative electrolyses. The

electrolytic compartments were separated by a ceramic diaphragm of porosity 2–3. As anode, the same ELTECH-chlorine/DSA[®] was used as previously and the cathodic material was Ti made. Various surface ratios ($1 < S_{\text{anode}}/S_{\text{cathode}} < 4$) are involved for the preparative electrolyses, carried out using a constant current electrochemical supplier (Iamvda 60 V/30A). The anolyte was supplied by solutions of (i) Brine (NaCl 300 g L⁻¹) and (ii) an acidic solution (HCl or H₂SO₄ 6 mol L⁻¹, according to the experiments, to maintain the anolyte pH < 3). A 'two push-syringes' device (model A-99 from Fischer Scientific) was used to supply these solutions at constant volumetric flow.

According to the operating conditions (pH, temperature, Cl⁻ concentration,...) various reactions could take place (1–12, Table 1).

Hypochlorite potentiometric titration was performed using an anhydrous sodium sulfite Na₂SO₃ (97%) according to the method described by Adam and Gordon [15]: reaction (13), Table 1.

By monitoring the zero current potential of a platinum electrode versus a Ag/AgCl/KCl_{saturated} reference electrode, the required volume of the sulfite solution to neutralize the hypochlorite and to access its concentration C_{ClO^-} can be determined.

The overall conversion X of the chloride ions for an electrolysis duration t (versus all the used volume of brine), as well as the corresponding Faradic yield y_f were calculated respectively by Eqs. (14) and (15):

$$X = \frac{\text{mol of Cl}^- \text{ transformed by electrolysis}}{\text{mol of Cl}^- \text{ (initial + introduced brine and acid)}}$$

$$X = \frac{2 * C_{\text{ClO}^-} * V_p}{(C_{\text{NaCl}} * V_{\text{anolyte}})^{\circ} + t * (Q_{\text{acid}} * C_{\text{acid}} + Q_{\text{brine}} * C_{\text{brine}})} \quad (14)$$

$$y_f = \frac{\text{produced mole number of OCl}^-}{\text{theoretical mole number of OCl}^- \text{ produced}} = \frac{C_{\text{ClO}^-} * V_p}{\frac{I_{\text{applied}} * t}{2 * F}} \quad (15)$$

where: V is the volume; V_p is the volume of the NaOH trapping solution of the produced gaseous chlorine (see corresponding section); C is the concentration; Q is the volumetric flow; I is the applied current and t the electrolysis duration.

3. Results

3.1. Electrochemical kinetics

To determine the appropriate current density to apply in order to carry out electrolyses in optimal conditions (no oxygen, no chlorate), current potential curves were plotted (Fig. 1) for various concentrations of sodium chloride (curves 1–4), with (a) and without (c) an electrolyte.

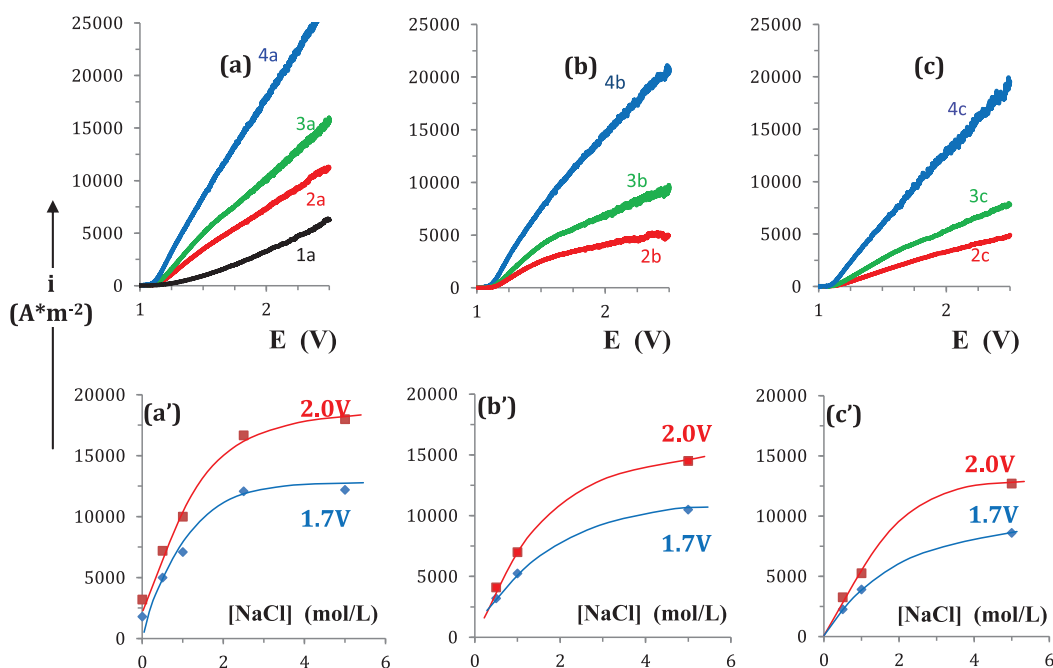


Fig. 1. Current potential curves obtained on chlorine/DSA® plate working electrode ($S = 24 \text{ mm}^2$), immersed in solutions containing various NaCl concentrations. Auxiliary electrode: Pt rod; Reference electrode: Ag/AgCl/KCl_{saturated}. Potential scan rate 5 mV s^{-1} ; Stirred solution; room temperature ($20 < T (\text{°C}) < 24$). 1: K_2SO_4 at 0.1 M; 2: NaCl 0.5 M; 3: NaCl 1 M; 4: NaCl 5 M; (curves 0.1 and 2.5 mol L^{-1} not represented). (a): Curves obtained with solutions containing K_2SO_4 0.1 M as supporting electrolyte. (b): Curves obtained from (a) after subtraction of the curve (1a) e.g. $i = i_{(\text{NaCl}+\text{K}_2\text{SO}_4)} - i_{(\text{K}_2\text{SO}_4)}$ (c): Curves obtained without additional electrolyte (simple brine solutions). (a'), (b') and (c'): Current densities measured at two potentials as a function of the NaCl concentration (extracted from (a–c) respectively).

The curves obtained without electrolyte (Fig. 1c), especially at chloride concentrations $< 1 \text{ M}$, present a pseudo plateau ($\sim 1.4 \text{ V} \sim 1.6 \text{ V}$); in the examined potential range, the curves do not show a clear exponential shape corresponding to water oxidation, meaning that the majority of the current is used for chloride oxidation. It is impossible to have a measure of the 'blank/residual current' in these conditions. Moreover, the current arises from migration and diffusion flux. At 2 V , current density reaches $\sim 5 \text{ kA m}^{-2}$, for 1 M NaCl solution alone (curve 3c).

Adding K_2SO_4 as supporting electrolyte enables the current used for water oxidation (curve 1a) to be estimated. Indeed, curves (b) were obtained from curves (2a to 4a) after subtraction of the curve (1a); this is the net current attributed to chloride oxidation, in presence of an electrolyte. These curves clearly indicate a plateau (mass transfer limitation) for $E > 1.4 \text{ V}$.

The rate of the oxidation of water at 2.4 V (curve 1a) appears to be significant for low concentrations of NaCl (50% of the overall current, curve 2a); it represents less than 20 % at high concentrations (curve 4a).

The net current densities, obtained for oxidation of chloride in presence of an electrolyte are higher than those measured in absence of K_2SO_4 ; for example, at 2 V , the ratio $i_{(3b)}/i_{(3c)}$ ($\sim 7 \text{ kA m}^{-2}$)/($\sim 5.2 \text{ kA m}^{-2}$) shows a current density $\sim 30\%$ higher for 1 M NaCl solution with K_2SO_4 .

Theoretically, (at the least for low NaCl concentrations, e.g. 1 M) the expected current in the 2c experiments has to be slightly higher than the current in the 2b experiments (and also for 2a), the K_2SO_4 ensuring part of the migration current. The general comparison of curves (2b–4b Fig. 1) with K_2SO_4 as supporting electrolyte and without K_2SO_4 (2c–4c Fig. 1), shows that for the same concentration of NaCl, the current is always higher, thus the K_2SO_4 appears to have an electrocatalytic effect on the chloride oxidation on the used DSA. Another explanation could be that K_2SO_4 causes the ionic conductivity of the solution to increase; consequently, for the same voltage, the current density increases.

Curves a', b' and c' (Fig. 1), indicate the current density evolution as a function of the sodium chloride concentration for potentials of the anode at 1.7 and 2 V/SCE . For all the curves, a non-linear variation was observed (especially for high NaCl concentrations). The main reasons could be: (i) the concentration is dependent on the diffusion coefficient and (ii) the effect of significant quantities of gaseous chlorine on the electrode surface could have led to a slight passivation of the anode.

The following equations provide the chloride concentration dependency on the magnitude of the current density at room temperature, for curves (c') obtained without an additional electrolyte, and corresponding to a conversion of chloride equal to zero (initial/input concentrations):

$$I_{\text{at } 1.7 \text{ V}} (\text{in } \text{A m}^{-2}) = 4532 \times C - 562.6 \times C^2 \quad R^2 = 0.999 \quad (16)$$

$$I_{\text{at } 2 \text{ V}} (\text{in } \text{A m}^{-2}) = 6171 \times C - 726.4 \times C^2 \quad R^2 = 0.998 \quad (17)$$

where C is the concentration of sodium chloride in the brine (mol L^{-1}).

For a supplying solution containing chloride at 5 mol L^{-1} , the initial admissible/maximal current density reaches 8.3 kA m^{-2} at 1.7 V and 12.5 kA m^{-2} at 2 V .

3.2. Reactor design

Fig. 2 describes the set-up designed for preparative electrolyses of chlorine. It is a divided asymmetric (glass made) cell, with volume compartments in the ratio: $V_{\text{anolyte}}/V_{\text{catholyte}} =$ from 1 to ~ 2). Only the anodic compartment was supplied both by brine and an acidic solution at constant volumetric flow ($Q_1 = Q_{\text{brine}} + Q_{\text{acid}}$, as required).

The electrolytic compartments were separated by a ceramic diaphragm; two different porosities (2/pores size in the range $100\text{--}200 \mu\text{m}$, and 3/pores size in the range $10\text{--}50 \mu\text{m}$) ceramic diaphragms were used to carry out the electrolyses; the goal here is to

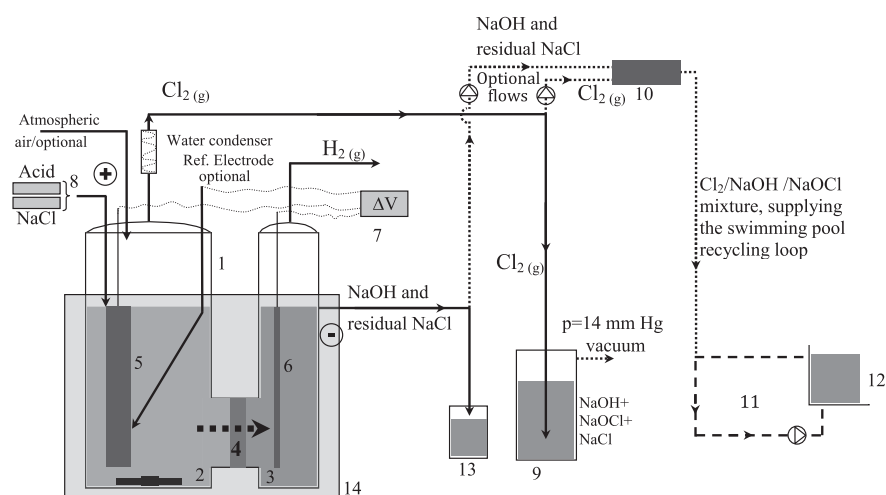


Fig. 2. Schematic representation of the experimental set-up used to carry out preparative electrolyses. 1: Electrochemical reactor (divided asymmetric electrolyzer); 2 and 3: anodic and cathodic compartments; 4: ceramic type diaphragm (porosity 2 or 3 depending on the experiments); 5 and 6: anode and cathode; 7: electrochemical power supplier; 8: push syringe supplier (two flows: brine and acid); 9: gaseous chlorine trapping solution (Cl_2 cumulates under NaOCl form in NaOH 5 mol L^{-1}); 10: absorber (chlorine by soda); 11: swimming pool recycling loop; 12: swimming pool; 13: waste; 14: immersion bath allowing partial regulation of the temperature of the reactor.

allow flow from the anodic to the cathodic compartment. Note that a Teflon porous diaphragm could also be used, in order to increase the life-time of the overall device.

Differences in the volumes of both compartments contribute to the reduction of the back-diffusion flux of species from the catholyte to the anolyte (especially convective flux), and consequently to avoid losses in the Faradic yield: indeed, high values of the ratio $V_{\text{anolyte}}/V_{\text{catholyte}}$ allows the velocity of the motion of the catholyte to the outlet of the compartment to be increased (comparatively to the velocity of the motion of the anolyte into the anodic compartment).

To produce gaseous chlorine (1) and to avoid hypochlorite formation (2), the pH of the brine in the anodic compartment must be kept at less than 3 [11]. Two possibilities were chosen here to supply the anodic compartment;

- the pH of the brine was adjusted to 3 (HCl or H_2SO_4) before introduction to the reactor,
- the brine and an acidic solution (HCl or H_2SO_4) supply the reactor simultaneously.

During electrolysis, the pH of the cathodic compartment increased, measured values were higher than 10. Dissolved chlorine (or hypochlorous acid as function of the pH), which appear in the anodic compartment, could cross the ceramic separator and move to the cathodic compartment, then they can be reduced to chloride ions. The consequence of these phenomena is the drop in the faradic yield of the system.

Note that (as a function of the operation), the reactor was immersed in a cold water bath (14). This is to avoid significant increases in temperature (as close to $<30 \text{ }^\circ\text{C}$ as possible) to avoid the generation of chlorates by secondary reactions [16].

Gaseous chlorine is produced at the anode according to the reaction (1), Table 1; even if the potential of this reaction is higher than the potential of the oxidation of the water, catalytic coating of the chlorine DSA enables the oxidation of the chloride with very satisfactory faradic yields.

Chlorine can follow two different circuits:

- Elements 10/11/12 of Fig. 2; Cl_2 could be introduced in the catholyte flow (NaOH + residual NaCl) using a fine porosity disperser; then absorption of chlorine can take place, followed by its disproportionation (reaction 12, Table 1)

leading to the hypochlorite formation. The resulting mixture was introduced within the liquid flowing in the swimming pool recycling loop; high flow in this recycling loop allows efficient gas/liquid transfer and rapid conversion of Cl_2 to hypochlorite.

- Element 9 of Fig. 2; in this study, in order to optimize the involved system, a Cl_2 trapping tank (absorption + disproportionation to hypochlorite) containing at the initial time concentrated NaOH solution (5 mol L^{-1}) was used. A second identical trapping tank was connected at the outlet of the first one, to retain the eventual unreacted chlorine.

3.3. Experimental optimization of the chloride conversion in the reactor

Various preparative electrolyses were performed to optimize the effect of the operating parameters (feed flow, S_a/S_c , T , acid nature and flow rate, ...) on the chloride conversion within the reactor. The mass balances were performed in both the anodic and the cathodic compartments, according to the analytical procedure previously described.

3.3.1. Effect of the residence time of the feeding solution on the steady state establishment

Galvanostatic electrolyses were performed using the set-up described in Fig. 2, supplied in the anodic compartment by two different solutions: the brine (NaCl , 5 mol L^{-1}) and hydrochloric acid (6 mol L^{-1}) for pH adjustment. The applied current density (1.69 kA m^{-2}) corresponds to an anodic potential in the range of 1 V/SCE, and the aim of these experiments is to estimate the time required to reach the steady state, in the cathodic compartment for the chloride ions. Three different experiments are performed for residence times (τ) in the anodic compartment of 1.1, 1.7 and 2.5 h respectively.

Produced chlorine, cumulated under NaOCl form in the 'gaseous chlorine trapping solution (element 9, Fig. 2)', was titrated according to the reaction (13), Table 1 (see Section 2). Simultaneously, chloride concentration within the cathodic compartment (and/or in the 'gaseous chlorine trapping solution (element 9, Fig. 2)') was determined by potentiometric titration by silver nitrate. Fig. 3 indicates the temporal evolution of both the residual concentration of Cl^- ions (a) and their conversion (b).

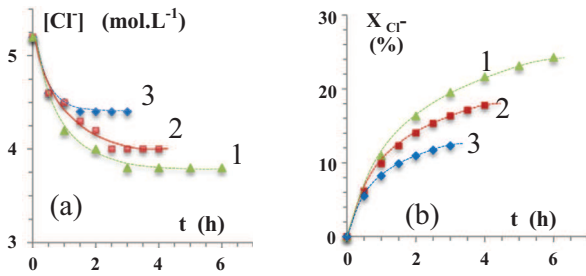


Fig. 3. Temporal evolution of both the concentration (a) of the chloride ion in the anolyte, and its conversion (b) in the outlet of the cathodic compartment, during galvanostatic electrolyses, for various feed solutions of brine ($C_{\text{NaCl}} = 5 \text{ M}$): Q_{NaCl} at 5 mol L^{-1} : 60, 85, 135 cm^3/h for curves 1 \blacktriangle , 2 \blacksquare and 3 \blacklozenge respectively. $i = 1.7 \text{ kA m}^{-2}$; $S_{\text{anode DSA Cl}} = 39 \text{ cm}^2$; $S_{\text{cathode Ti}} = 19 \text{ cm}^2$; $V_{\text{anodic compartment}} = 150 \text{ cm}^3$; $T \sim 30 \text{ }^\circ\text{C}$ (as possible).

Results showed that at a constant flow rate, the concentration of the chloride ion in the anolyte (a) decreases with time to reach a quasi constant value (steady state). Let us note that the steady state concentration of chloride increases with the flow, showing non optimized operating conditions. Permanent regime is reached after durations in the range from 1.5 to 3 h, depending on the residence time of the feeding solution. Usually the time t required to reach steady state conditions (e.g. here a chloride constant concentration) must be low in comparison to the duration of the overall process, approx. 1- or 2-fold of the residence time.

Fig. 3/graph (b) shows the corresponding chloride conversion to hypochlorite. As expected, at a constant flow rate, obtained conversion increases over time for all the examined volumetric flow rates; nevertheless, the maximal conversion reached remains low ($\sim 30\%$ for $60 \text{ cm}^3/\text{h}$) and decreases until $\sim 10\%$ when the flow increases approximately twofold, indicating that under such conditions, all the examined volumetric flow are high and inappropriate to the request application (conversion $>75\%$ for faradic yield close to 90%). It can be noted that the conversion value can be increased simply by applying higher current density values, in accordance with values determined by the $I=f(E)$ curves of Fig. 1 (or the two Eqs. (14) and (15) corresponding to the potentials of the anode 1.7 and 2 V/SCE).

3.3.2. Effect of the applied current density on electrolyses performance

The effect of the applied current density on both the chlorine production and the faradic yield (y_f) was examined by preparative electrolyses, carried out under low volumetric flow (residence time of the anolyte $\tau = 5 \text{ h}$; $V_{\text{anodic compartment}} = 150 \text{ cm}^3$); the results are indicated in Fig. 4.

(i) For short electrolysis durations ($<5 \text{ h}$), curves (a) of Fig. 4, show that, chlorine production (measured at time t , in the chlorine

trapping solution, element 9, Fig. 2) linearly increases over time, for all the applied current densities; simultaneously, in the examined range of $1.2\text{--}2.1 \text{ kA m}^{-2}$, the faradic yield remains higher than 90% (curves (b), Fig. 4), meaning that, all the current was used for chloride oxidation; the applied current density remains lower than the maximal admissible. Moreover, despite the relatively high residence time ($3\text{--}4 \text{ h}$) of solution in the reactor, the obtained faradic yields ($\sim 90\%$) demonstrate a minor effect of the back-diffusion flux of the species from the catholyte to the anolyte. Indeed OH^- produced in the cathodic compartment and transferred (migration/back diffusion) to the anodic one, could cause production of ClO^- instead of Cl_2 ; hypochlorite could be transferred by convective flow to the cathodic compartment and could be reduced, causing the faradic yield to decrease.

For higher durations, both the chlorine production rate and the faradic yield decrease meaning that part of the current was used to oxidize water and to produce the oxygen.

The slopes (s) of the straight lines of curves (a) of Fig. 4, indicated in Fig. 5, can be used to determine the Cl_2 moles number, absorbed and transformed to hypochlorite, in the trapping solution $n_{\text{Cl}_2(\text{in mol})} = 0.25 \times s \times t$ (in h) for any electrolyses duration $t < 5 \text{ h}$ (Fig. 5). Then, the empiric Eq. (18) 'mole number of the produced chlorine at time t , versus the applied current density' was established using the graph in Fig. 5.

$$\{0.25 \times s \times t\}_{\text{mol of produced Cl}_2} = 8.3 \times 10^{-5} \times i - 1.1 \times 10^{-8} \times i^2 \quad R^2 = 0.989 \quad (18)$$

(ii) For electrolyses of longer duration ($5\text{--}6 \text{ h}$), losses in current are more significant, especially for the highest applied current density. Fig. 4(c) confirms these results; indeed for 6 h electrolyses duration, increasing the applied current density by 2-fold ($1.3 \rightarrow 2.8 \text{ kA m}^{-2}$, so $\sim 120\%$) causes the conversion to increase by about 65% (from 30% to 50%); the quantity of chlorine produced (cumulated under NaOCl form in the 'gaseous chlorine trapping solution 250 ml of the NaOH (element 9, Fig. 2)') is in the range of $2.1\text{--}3.5 \text{ mol L}^{-1}$. In addition, applying high current densities could contribute to the acceleration of the degradation of the catalytic coating of the DSA, so this parameter needs optimizing (see follow §).

To sum up, steady state seems to be achieved at about 6 h (Fig. 4c), and for these experiments, only current densities lower than around 1.5 kA m^{-2} offers faradic yields higher than 90% for chloride conversions in the range of $35\text{--}40\%$.

3.3.3. Effect of the working electrode area on chlorine production

The effect on chlorine production of the geometric area of the anode was examined by three preparative electrolyses achieved under low volumetric flow ($\tau = 5 \text{ h}$). To operate with the same

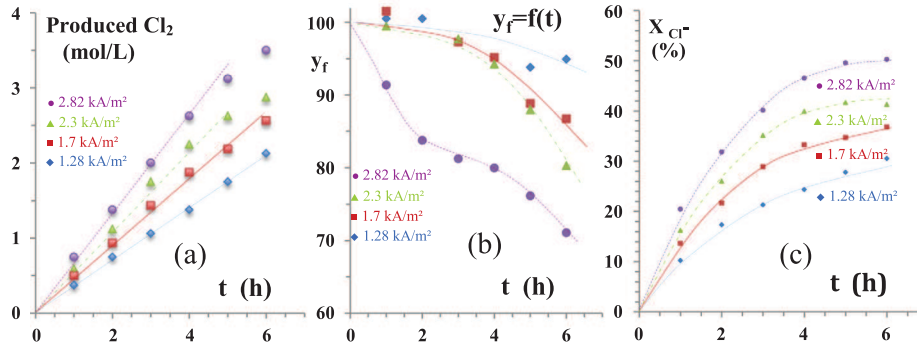


Fig. 4. Results of galvanostatic electrolyses performed under various applied current densities i : (\blacklozenge) 1.28 , (\blacksquare) 1.7 , (\blacktriangle) 2.3 and (\bullet) 2.8 kA m^{-2} respectively. $S_{\text{anode DSA Cl}} = 39 \text{ cm}^2$; $S_{\text{cathode Ti}} = 19 \text{ cm}^2$; $V_{\text{anodic compartment}} = 150 \text{ cm}^3$; $T \sim 30 \text{ }^\circ\text{C}$ (as close as possible); Q_{NaCl} at 5 mol L^{-1} : $15 \text{ cm}^3/\text{h}$. (a): Temporal evolution of chlorine cumulated under NaOCl form in the 'gaseous chlorine trapping solution (250 cm^3 of NaOH , element 9, Fig. 2)'; (b) Faradic yield evolution, (c) Chloride ion conversion; Q_{HCl} at 6 mol L^{-1} for (a-c) = $15 \text{ cm}^3/\text{h}$.

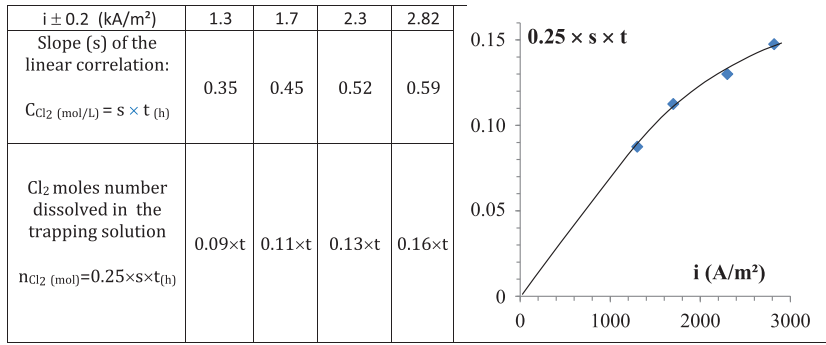


Fig. 5. Empirical correlations providing produced chlorine Cl₂ moles number dissolved in the trapping solution, as a function of both the electrolysis duration and the current density (results extracted from Fig. 4).

current density (1.70 kA m⁻²) for all electrolyses, the applied current was adjusted versus the electrochemical area of the electrode according ($I_{(A)} = 0.17 \times S_{(cm^2)}$). Three identical grids of DSA-Cl were used to vary the area of the anode; one grid/39cm², two or three sandwiched grids for respectively 59 and 79 cm².

Results are indicated in Fig. 6. As previously (Fig. 4(a)), for low electrolysis durations (~4 h), curves show that chlorine production linearly increases with time (for all electrolyses achieved), meaning that, despite the high residence time of solution in the reactor, all the current was used for chloride oxidation; the applied current remains lower than the maximal admissible. For electrolyses of longer duration, chlorine production rates decrease, implying losses in current, and probably a partial back diffusion.

Increasing the applied current from ~6.6 A (39 cm²) to ~10 A (59 cm²) causes the chlorine concentration (and chloride conversion) to increase (Fig. 6); nevertheless, for the electrolysis involving 3 sandwiched grids as anode and a current of ~13.5 A, chlorine production remains lower than that obtained by the second electrolyse. On the simple basis of the use of the applied current, there is no reason to obtain a lower quantity of chlorine; even if the faradic yield decreases, the quantity of chlorine has to be at the least, the same as that obtained for surfaces area anode equal to 59 cm². The following explanations could justify this behavior:

(i) for this kind of system involving juxtaposition of three grids, the first electrode absorbs a larger fraction of the current, the other grids being located behind the first anode; practically, this does not work; this implies significant current densities on the first electrode and consequently secondary reaction (water oxidation, chlorates) leading to losses in the faradic yield. The consequence of this is the impossibility to use several layers of the expanded metal (simply sandwiched) as anode, to increase chlorine production.

(ii) The ceramic diaphragm used for this reactor (porosity 3), causes an ohmic drop, leading to a significant increase in

temperature (60 °C) which favors secondary-type products (chlorates). Moreover, ceramic used could locally dissolve under the temperature effect, leading to the mixing of solution and loss in production (Teflon porous diaphragm is preferable).

3.3.4. The effect of other parameters on the chlorine production

This section presents electrolyses that are expected to show the effects of both temperature and the acidic nature on the electrolyse performances (conversion and yield).

(i) Electrolyses were carried out for three temperatures: $20 < T^{\circ}C \lesssim 30$, $30 < T^{\circ}C \lesssim 45$ and $40 < T^{\circ}C \lesssim 55$. Unfortunately local values of temperature, especially at the electrodes and at the ceramic diaphragm, could be higher, due to a low efficiency of the 'temperature-regulation' system (cold water added periodically in the immersion bath-element 14, Fig. 2). All other conditions are those indicated in Fig. 4 at 1.7 kA m⁻².

The results show for all the electrolyses (and especially for electrolyses durations <4 h), the same linear evolution of the chlorine production {chlorine cumulated under NaOCl form in the 'gaseous chlorine trapping solution (element 9, Fig. 2)'} over time, according to the following equation:

$$C_{Cl_2}(\text{mol L}^{-1}) = 0.435 \times t_{(h)} \text{ for } 20 < \forall T^{\circ}C < 50 \quad (19)$$

To conclude, in the examined range ($20 < \forall T^{\circ}C < 50$; $i = 1.7 \text{ kA m}^{-2}$) and for relatively short electrolyses durations (<4 h; $X_{Cl^-} < 50\%$) temperature does not have an effect on the faradic yield nor the chloride conversion.

For higher electrolyses durations or higher temperatures, results show a non-linear evolution of the chlorine production over time; side products could appear (chlorates, O₂), and mixing of the anolyte with the catholyte could cause the losses of the faradic yield and the non-linear increase of the chloride conversion over time.

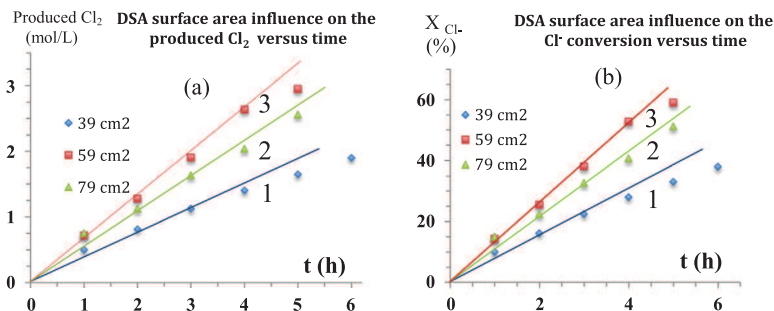


Fig. 6. Results of galvanostatic electrolyses performed using various electrochemical surface area anodes: $S_{\text{anode DSA Cl}}$: 39, 59 and 79 cm² for curves 1♦, 2■ and 3▲ respectively; $S_{\text{cathode Ti}} = 19\text{cm}^2$; $i_{\text{anode}} = 1.7 \text{ kA m}^{-2}$; $V_{\text{anodic compartment}} = 150 \text{ cm}^3$; Q_{HCl} at 6 mol L⁻¹ = Q_{NaCl} at 5 mol L⁻¹: 15 cm³/h; ($30 < T^{\circ}C \lesssim 45$, as close as possible). (a): Temporal evolution of chlorine cumulated under NaOCl form in the 'gaseous chlorine trapping solution (9, Fig. 3)'; (b): Temporal evolution of the conversion of the chloride ions.

(ii) This concerns the effect of the acidic nature added to the anodic compartment; both sulfuric and hydrochloric acids were used, for the same volumetric flow and concentration, to maintain acidic conditions in the anodic compartment (due to back diffusion/migration of OH^- from the cathodic compartment). Three different sets of experiments were performed by varying the current density and using alternatively HCl or H_2SO_4 . For both acids, the results, indicated in Fig. 7(a), do not show significant differences in the produced quantity of chlorine: its concentration practically linearly varies versus time for short/ ~ 4 h electrolysis durations, meaning that:

- applied current density remains lower than the maximal admissible,
- the anion SO_4^{2-} does not affect the kinetics of the system Cl^-/Cl_2 ,
- HCl introduced in the anodic compartment, brings the required proton molar flux to maintain a constant pH and to avoid production of NaOCl directly at the electrode; consequently, the use of sulfuric acid (which provide two H^+ /mole) can be avoided.

The plot (b) of Fig. 7 shows the temporal evolution of the chloride ions conversion; conversion appears to be higher when sulfuric acid was used because the depletion of the chloride concentration in the anolyte is faster; indeed, adding H_2SO_4 causes the dilution of Cl^- ions in the anolyte, while HCl provides the same quantity of chloride as NaCl.

Let us note that use of sulfuric acid causes interferences in the potentiometric titration of chloride ions by Ag^+ , and implies the use of other techniques (Ionic liquid chromatography), so we choose to use hydrochloric acid to control the pH of the anolyte.

3.4. Determination of the theoretical profiles of Cl_2 concentration and Cl^- conversion and comparison with the experimental evolutions

In order to formulate a predictive tool to optimize the proposed divided and stirred electrochemical reactor (Fig. 2) for swimming pools, complete macroscopic mass balances were written for various species present in both anodic and cathodic compartments. All the parameters used were defined in Appendix 2/Nomenclature. Resolution of the obtained equation system (Appendix 1) enables obtaining theoretical concentration profiles, here mainly hypochlorite/chlorine and chloride, and performing comparison between experimental and theoretical conversion/concentrations, in order to validate the theoretical model.

3.4.1. Mass balance

Reactions which take place within the reactor are:

On the anode: (1) and as side reaction (3), Table 1.

On the cathode: (5) or, as function of the pH (6), Table 1.

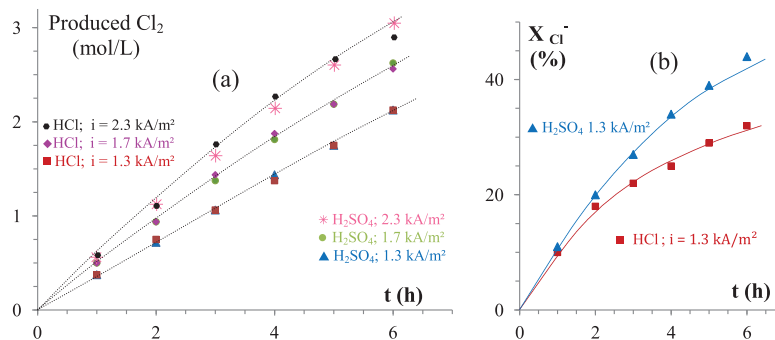


Fig. 7. Effect of both the acidic nature and the applied current density on the temporal evolution of: (a): Cl_2 cumulated under NaOCl form in the 'gaseous Cl_2 trapping solution (element 9, Fig. 2)'. (b): Cl^- conversion. Q_{acid} at $6 \text{ mol L}^{-1} = Q_{\text{NaCl}}$ at 5 mol L^{-1} : $15 \text{ cm}^3/\text{h}$. $S_{\text{anode DSA Cl}} = S_{\text{cathode Ti}} = 39 \text{ cm}^2$; $V_{\text{anodic compartment}} = 150 \text{ cm}^3$; $30 < T^\circ\text{C} \leq 45$.

The overall mass balance equation for a specie can be written in terms of molar flux (mol s^{-1}) as follow:

Input flux – output flux = Reaction flux + accumulation flux + migration/convection/diffusion across the ceramic diaphragm flux + loss by gas (H_2 and /or Cl_2) distillation

$$F_{in} - F_o = F_r + F_{acc} + F_m + F_c + F_D + F_{loss} \quad (20)$$

On the anodic compartment, this can be made explicit as follows:

$$(QC)_{inlet} - (QC)_{outlet} = \pm \frac{y_f I}{nF} + V_a \frac{dC}{dt} \pm \frac{t_j I}{nF} + Q_d C \pm S_d D \text{grad} C + \text{loss} \quad (21)$$

where: C: molar concentration (mol m^{-3}); D: diffusion coefficient ($\text{m}^2 \text{s}^{-1}$); F: Faraday constant (C mol^{-1});

I: current (A); n: electron number; Q: volumetric flow ($\text{m}^3 \text{s}^{-1}$); S_d geometric area of the ceramic diaphragm; t_j is the transference number of specie $j = \frac{z_j^2 F^2 C_j u_j}{\sum_j z_j^2 F^2 C_j u_j}$; t: time (s); z_j : valence number of specie j ; u_j : ionic mobility of the ion j ($\text{m}^2 \text{s}^{-1} \text{V}^{-1}$); V: volume (m^3); y_f : faradic yield (%).

Resolution of mass balance equations for chloride ions on both the anodic and the cathodic compartments (these equations are dependent, see Appendix 1) was performed by an iterative method for various time steps: e.g. for the first step (1 h electrolysis duration), first equation was solved assuming the other concentration constant, then knowing the conversion, the second concentration can be calculated by solving the second equation for the next step (see Appendix 1).

The appendix also presents the mass balance equations for other species: water, cumulated NaOCl, H^+ , (resolution not presented).

$$X = \left(1 + \frac{\frac{I}{nF}(y_f - t_{\text{Cl}^-}) - Q_1 C^0 - Q' C' - D_{\text{Cl}^-} \frac{S_d}{\ell} C_3}{(Q_2 + D_{\text{Cl}^-} \frac{S_d}{\ell}) C_{in}} \right) \times \left(1 - \exp - \frac{Q_2 + D_{\text{Cl}^-} \frac{S_d}{\ell}}{V_a} t \right) \quad (22a)$$

The expression providing the concentration of chloride ions in the outlet of the reactor is given by:

$$[\text{Cl}^-]_{\text{cathodic compartment}} = C_3(t) = \frac{S_k s - \frac{I t_{\text{Cl}^-}}{nF}}{Q_2 + \frac{D_{\text{Cl}^-} S_d}{\ell}} \left[1 - \exp - \frac{Q_2 + \frac{D_{\text{Cl}^-} S_d}{\ell}}{V_c} t \right] + C_{in}(1 - X) \quad (22b)$$

3.4.2. Comparison between theoretical and experimental results

Comparison between theoretical and experimental temporal evolution of the chloride conversion was achieved for galvanostatic

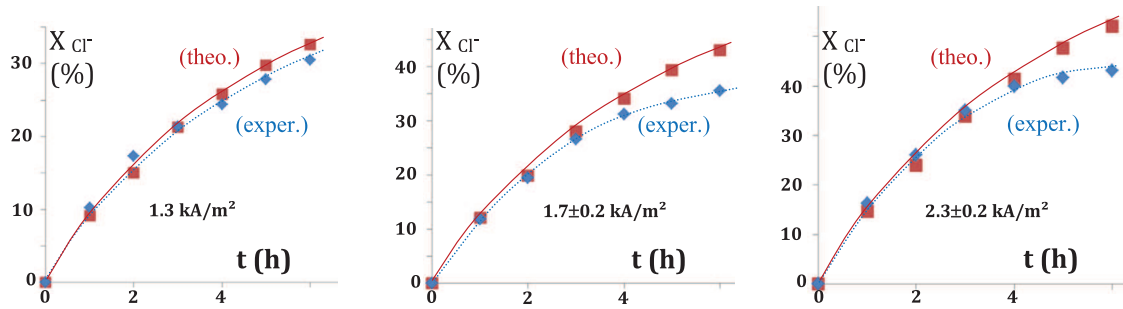


Fig. 8. Comparison between theoretical \blacksquare and experimental \blacklozenge temporal evolution of the chloride conversion for galvanostatic electrolyses conducted, under three current densities. $V_{\text{anolyte}} = 150 \text{ cm}^3$; $V_{\text{catholyte}} = 90 \text{ cm}^3$; y_F assumed: 100%; $C_{\text{acid}} = C = 16 \text{ mol L}^{-1}$; $C_{\text{NaCl}} = C^0 = 5 \text{ mol L}^{-1}$; $s_{\text{Cl}_2} = 0.08 \text{ mol L}^{-1}$; $Q_{\text{NaCl}} = Q_{\text{acid}} = 15 \text{ cm}^3/\text{h}$; $S_{\text{anode DSA}} = S_{\text{cathode Ti}} = 39 \text{ cm}^2$; $S_d = 1.25 \cdot 10^{-3} \text{ m}^2$; $\ell = 4 \text{ mm}$; Parameters used for the calculation of the theoretical conversion: $k = 1.76 \cdot 10^{-6} \text{ m s}^{-1}$; Diffusion coefficients (in $\text{m}^2 \text{ s}^{-1}$): $\text{H}^+ = 9.3 \cdot 10^{-9}$; $\text{Cl}^- = 2.0 \cdot 10^{-9}$; $30 < T^\circ\text{C} \leq 45$; Mobilities (in $\text{m}^2 \text{ s}^{-1} \text{ V}^{-1}$): $\text{Na}^+ = 5.2 \cdot 10^{-8}$; $\text{Cl}^- = 7.9 \cdot 10^{-8}$; $\text{H}^+ = 3.6 \cdot 10^{-7}$; $\text{HO}^- = 2.10^{-7}$.

electrolyses, conducted under three current densities. Data, parameters and results are summarized in Fig. 8.

Obtained theoretical results correlate with the experimental one ($\Delta X < 2\%$ for $t = 4 \text{ h}$), for the lowest current density (1.3 kA m^{-2}), that confirms the validity of the theoretical approach.

Discrepancies between theory and experience arise for electrolysis durations greater than 3 h, and for higher current densities (at 6 h, ΔX reaches $\sim 8\%$ and $\sim 10\%$ for 1.7 and 2.3 kA m^{-2} respectively); theoretical conversion is $\sim 10\%$ higher than the experimental one (which reaches 43%). These differences were due to the fraction of the current used for water oxidation when chloride concentration decreases, and the potential of the anode increases. Indeed, under 2.3 kA m^{-2} , after 6 h electrolysis, the experimental conversion of chloride reaches 43% and the potential of the anode is in the range of $1.2 \text{ V}/\text{Ag}/\text{AgCl}/\text{Cl}^-$. This value correlates with the potential measured on the $i = f(E)$ curve (Fig. 1) obtained with 2.5 M of NaCl ($\sim 50\%$ of conversion/similar to the 43% obtained under 2.3 kA m^{-2}).

To reduce discrepancies between theoretical and experimental results, it will be interesting to take account of the kinetic law of water oxidation in the various mass balances previously established.

4. Conclusion

The aim of the achieved study was to design and to optimize an electrochemical reactor for the chlorination of swimming pools, operating without electrodes polarity inversion.

Plotting of current potential curves for various conditions allows empiric equations to be established providing the chloride concentration dependence on the magnitude of the initial current density, and to select the current to apply in order to operate under favorable faradic yield conditions.

The proposed two-compartment asymmetric electrochemical reactor treats concentrated brine elaborated with demineralized water (no limescale); this acidified brine solution feeds the anodic compartment and after electrolysis solution moves to the cathodic one crossing the ceramic diaphragm. Gaseous chlorine, produced in the anode and absorbed in the alkalized catholyte (in the outlet of the cathodic compartment), provides the hypochlorite solution. The overall low cost device is simple and can be operated automatically without specific treatment.

Experimental optimization of the effect of the various operating parameters for the chlorine production was achieved, and results show that concentrated brine could treat with a chloride conversion close to 50% in a few hours. The faradic yields remain higher than 80%. Ratios of $V_{\text{anolyte}}/V_{\text{catholyte}}$ higher than 2 could increase the obtained chloride conversion. Besides, a controlled porosity

Teflon disk could easily replace the ceramic diaphragm used, to increase the life-time of the overall device. Achieved chlorine production reaches $1 \text{ kmol}/\text{day}/\text{m}^2$ and $4 \text{ mol}/\text{day}$ for the present device; respecting the defined operating parameters, the extrapolation of the proposed device in the appropriate scale does not present difficulties.

Macroscopic mass balance, taking into account the various transfers arising in the reactor (including losses and back diffusion) was performed and the obtained theoretical results correlate with the experimental ones ($X_{\text{theor. Cl}^-} - X_{\text{exper. Cl}^-} < 10\%$).

Acknowledgements

We would like to thank the 'BIOPOOL Company France' and the 'Région Midi-Pyrénées' for financial support during this work. Thanks are also due to Pr. L. Arurault (CIRIMAT, UPS), B. Joyeux (BIOPOOL) and N. Noel (BIOPOOL) for helpful discussions and to Sophie Chambers for checking the manuscript.

Appendix 1

A.1. Mass balance for chloride ions on the anodic compartment

Mass balance requires the estimation of the transference number of Cl^- :

$$t_{\text{Cl}^-} = \frac{C(t)u_{\text{Cl}^-}}{C(t)u_{\text{Cl}^-} + [\text{H}^+]u_{\text{H}^+} + [\text{Na}^+]u_{\text{Na}^+}}$$

Using the following values for mobilities ($10^{+8} \times u_{\text{in}} \text{ m}^2 \text{ s}^{-1} \text{ V}^{-1}$): $\text{Na}^+ = 5.2$; $\text{Cl}^- = 7.9$; $\text{H}^+ = 36$.

Because the concentration of Cl^- varies versus time, t_{Cl^-} was calculated at the beginning and the end of the electrolysis and the average value, calculated as follows, was assumed to be constant.

$t = 0$;	$[\text{Cl}^-] = [\text{Na}^+] = 5 \text{ kmol}/\text{m}^3$;	$\Rightarrow t_{\text{Cl}^-} = 0.6$	$\Rightarrow t_{\text{Cl}^- \text{ average}} = 0.52$
$X = 0\%$.	$[\text{H}^+] = 1 \text{ mol}/\text{m}^3$		
$t = 6 \text{ h}$;	$[\text{Cl}^-] = 2.5 \text{ kmol}/\text{m}^3$;	$\Rightarrow t_{\text{Cl}^-} = 0.43$	
$X \sim 50\%$	$[\text{Na}^+] = 5 \text{ kmol}/\text{m}^3$;		
	$[\text{H}^+] = 1 \text{ mol}/\text{m}^3$		

Chloride input flux corresponds to the introduction of both sodium chloride ($Q_1 C^0$) and hydrochloric acid ($Q' C'$) required to maintain a constant pH: $F_{\text{in}} = Q_1 C^0 + Q' C' = (Q_1 + Q') C_{\text{in}}$

where: C_{in} = overall input concentration of chloride in the anodic compartment.

Chloride output flux across the diaphragm corresponds to:

$$F_o = Q_2(1 - X)C_{in} = Q_2 \left(\frac{Q_1 C^o + Q' C'}{Q_1 + Q'} \right) (1 - X)$$

where X is the overall conversion of Cl^- .

Flux of reaction (oxidation), migration (to the cathodic compartment) and diffusion (from the cathodic to the anodic compartment) are respectively: $F_r = \frac{I}{nF} y_f$; $F_m = -t_{Cl^-} \frac{I}{nF}$ and $F_D = -D_{Cl^-} \frac{S_d}{\ell} (C_3 - C_{in}(1 - X))$.

Unidirectional diffusion was assumed to involve across diaphragm (surface area S_d ; thickness ℓ).

The volume of the anodic compartment (V_a) is constant and equal to the initial volume (V_a^o); indeed the height of the anodic compartment is similar to the height of the cathodic one, and regulated by the outlet in the cathodic compartment. So $V_a + (Q_1 + Q')t - Q_2t - tQ_3 = V_a^o$

where: Q_2t and Q_3t are respectively the volumes of solution leaving the anodic compartment by convection and removed by stream distillation (Cl_2).

Accumulation flux: $F_{acc} = \frac{dn}{dt} = V_a \frac{dC}{dt} = V_a \frac{d(1-X)C_{in}}{dt} = -C_{in} V_a \frac{dX}{dt}$

Finally, mass balance for Cl^- in the anodic compartment (Eq. (21)) can be written as:

$$\begin{aligned} & Q_1 C^o + Q' C' - Q_2 C_{in}(1 - X) \\ &= \frac{I}{nF} (y_f - t_{Cl^-}) - D_{Cl^-} \frac{S_d}{\ell} (C_3 - C_{in}(1 - X)) - C_{in} V_a \frac{dX}{dt} \end{aligned}$$

And after rearrangement of the previous equation:

$$\frac{dX}{dt} + \frac{Q_2 + D_{Cl^-} \frac{S_d}{\ell}}{V_a} X = \frac{\frac{I}{nF} (y_f - t_{Cl^-}) - Q_1 C^o - Q' C' - D_{Cl^-} \frac{S_d}{\ell} C_3(t)}{V_a C_{in}} + \frac{Q_2 + D_{Cl^-} \frac{S_d}{\ell}}{V_a} \quad (23)$$

A.2. Mass balance for chloride ions on the cathodic compartment

Chloride input flux corresponds to the transfer of the solution from the anodic compartment across the diaphragm:

$$F_{input \text{ cath. comp.}} = Q_2(1 - X)C_{in} = Q_2 \left(\frac{Q_1 C^o + Q' C'}{Q_1 + Q'} \right) (1 - X)$$

Chloride output flux: $F_o = Q_5 C_3$

Flux of migration (to the anodic compartment), diffusion (from the cathodic to the anodic compartment) and accumulation are respectively: $F_m = t_{Cl^-} \frac{I}{nF}$, $F_D = D_{Cl^-} \frac{S_d}{\ell} (C_3 - C_{in}(1 - X))$ and $F_{acc} = V_c \frac{dC_3}{dt}$

Reduction of dissolved chlorine (solubility s_{Cl_2}) in the solution supplied by the anodic compartment, produces chloride with the $F_r = -\frac{I_{lim \text{ of } Cl_2}}{nF} = -\frac{nFSD \text{ of } Cl_2}{nF\delta} = -Sk s_{Cl_2}$ where k is the mass transfer coefficient.

Current potential curves plotted for chlorine (hypochlorite in fact at 1%, curves not shown here) was used to get a rough estimation of the mass transfer coefficient: $k = 1.7610^{-6} \text{ m/s}$.

Mass balance chloride ions on the cathodic compartment can be written:

$$Q_2(1 - X)C_{in} - Q_2 C_3 = t_{Cl^-} \frac{I}{nF} + D_{Cl^-} \frac{S_d}{\ell} (C_3 - C_{in}(1 - X)) + V_c \frac{dC_3}{dt} - Sk s_{Cl_2}$$

After rearrangement and simplification of the previous equation can be written:

$$\frac{dC_3}{dt} + \frac{Q_2 + D_{Cl^-} \frac{S_d}{\ell}}{V_c} C_3 = + \frac{Q_2 + D_{Cl^-} \frac{S_d}{\ell}}{V_c} C_{in} - \frac{Q_2 + D_{Cl^-} \frac{S_d}{\ell}}{V_c} C_{in} X + \frac{S_{Cl_2} k}{V_c} s - \frac{t_{Cl^-} I}{nF} \quad (24)$$

Eqs. (23) and (24) are dependant. They can be solved by iterative method for various time steps: e.g. for the first step (1 h electrolysis duration), Eq. (23) was solved assuming C_3 constant. Then knowing X , C_3 can be calculated by solving Eq. (24) for the next step.

So, solution of Eq. (23) with $C_3 = \text{Constant}$ can be written as:

$$X = K \exp \left(-\frac{Q_2 + D_{Cl^-} \frac{S_d}{\ell}}{V_a} t \right) + \frac{\frac{I}{nF} (y_f - t_{Cl^-}) - Q_1 C^o - Q' C' - D_{Cl^-} \frac{S_d}{\ell} C_3}{(Q_2 + D_{Cl^-} \frac{S_d}{\ell}) C_{in}} + 1$$

where K is a constant determined using the initial conditions:

$$\text{at } t = 0 \rightarrow X = 0 = K + \frac{\frac{I}{nF} (y_f - t_{Cl^-}) - Q_1 C^o - Q' C' - D_{Cl^-} \frac{S_d}{\ell} C_3}{(Q_2 + D_{Cl^-} \frac{S_d}{\ell}) C_{in}} + 1$$

$$\rightarrow K = -1 - A \text{ where } A = \frac{\frac{I}{nF} (y_f - t_{Cl^-}) - Q_1 C^o - Q' C' - D_{Cl^-} \frac{S_d}{\ell} C_3}{(Q_2 + D_{Cl^-} \frac{S_d}{\ell}) C_{in}}$$

Substitute in the previous solution led to:

$$X = (1 + A) \left(1 - \exp \left(-\frac{Q_2 + D_{Cl^-} \frac{S_d}{\ell}}{V_a} t \right) \right)$$

$$\text{Finally: } [Cl^-]_{\text{cathodic compartment}} = C_3 = C_{in}(1 - X) = C_{in} \left[-A + (A + 1) \exp \left(-\frac{Q_2 + D_{Cl^-} \frac{S_d}{\ell}}{V_a} t \right) \right]$$

Concerns Eq. (24), for the corresponding step and X (e.g. $C = C_{in}(1 - X)$), we can write:

$$\frac{dC_3}{dt} + \frac{Q_2 + D_{Cl^-} \frac{S_d}{\ell}}{V_c} C_3 = + \frac{Q_2 + D_{Cl^-} \frac{S_d}{\ell}}{V_c} C_{in}(1 - X) + \frac{Sk}{V_c} s - \frac{t_{Cl^-} I}{nF}$$

So, solution of this Eq. (24), assuming $C = C_{in}(1 - X)$ constant in the corresponding step, can be written as:

$$C_3(t) = K' \exp \left(-\frac{Q_2 + D_{Cl^-} \frac{S_d}{\ell}}{V_c} t \right) + \frac{Sks - \frac{I t_{Cl^-}}{nF}}{Q_2 + D_{Cl^-} \frac{S_d}{\ell}} + C_{in}(1 - X)$$

K' was determined using the initial condition:

$$\text{At } t = 0; C_3 = C^o \rightarrow C_3 = K' + \frac{Sks - \frac{I t_{Cl^-}}{nF}}{Q_2 + D_{Cl^-} \frac{S_d}{\ell}} + C^o \rightarrow K' = -\frac{Sks - \frac{I t_{Cl^-}}{nF}}{Q_2 + D_{Cl^-} \frac{S_d}{\ell}}$$

$$\text{Finally } C_3(t) = \frac{Sks - \frac{I t_{Cl^-}}{nF}}{Q_2 + D_{Cl^-} \frac{S_d}{\ell}} \left[1 - \exp \left(-\frac{Q_2 + D_{Cl^-} \frac{S_d}{\ell}}{V_c} t \right) \right] + C_{in}(1 - X)$$

For other species, mass balance was written as follow (equations were not solved):

A.3. Mass balance for water on the anodic compartment

$$F_{in} - F_o = F_r + F_{acc} + F_{loss} \rightarrow \frac{Q_1 \rho}{M(H_2O)} - \frac{Q_2 \rho'}{M(H_2O)} = \frac{(1 - y_f) I}{nF} + \alpha \frac{I}{nF}$$

A.4. Mass balance for water on the cathodic compartment

$$F_{in} - F_o = F_r + F_{loss} \rightarrow \frac{Q_2 \rho'}{M(H_2O)} - \frac{Q_5 \rho''}{M(H_2O)} = \frac{I}{2F} + \beta \frac{I}{2F}$$

A.5. Mass balance for cumulated NaOCl in the 'gaseous chlorine trapping solution (250 ml of 5M NaOH; Fig. 2 elem. 9)

$$F_{in} - F_o = F_r + F_{acc} \rightarrow 0 = -\frac{I}{nF} + (V_p + Q_3 t) \frac{d[ClO^-]}{dt}$$

Reaction here corresponds to the 'instantaneous' disproportionation of chlorine (11) in alkali media

A.6. Mass balance for hydrogen ions (H^+) on the anodic compartment

$$F_{in} - F_o = F_r + F_m + F_{acc} + F_D \rightarrow Q_a C' - Q_2 C'' = -\frac{I(1-y_f)}{nF} + t_{H^+} \frac{I}{nF} + V_a \frac{dC'}{dt} - D_{H^+} \frac{S_d}{\ell} (C' - C'')$$

which can be rearranged as follows: $\frac{dC'}{dt} + \left(\frac{Q_2 + D_{H^+} \frac{S_d}{\ell}}{V_a} \right) C' = \frac{Q_a C' - t_{H^+} \frac{I(1-y_f)}{nF} + D_{H^+} \frac{S_d}{\ell} C''}{V_a}$

Solution of this equation is: $C''(t) = K \exp\left(-\frac{Q_2 + D_{H^+} \frac{S_d}{\ell}}{V_a} t\right) + \frac{Q_a C' - t_{H^+} \frac{I(1-y_f)}{nF} + D_{H^+} \frac{S_d}{\ell} C''}{Q_2 + D_{H^+} \frac{S_d}{\ell}}$

where K determined from the initial conditions: $C''(0) = C' \Rightarrow K = C' - \frac{Q_a C' - t_{H^+} \frac{I(1-y_f)}{nF} + D_{H^+} \frac{S_d}{\ell} C''}{Q_2 + D_{H^+} \frac{S_d}{\ell}}$

Final solution can be written as:
 $[H^+]_{\text{anodic compartment}} = C''(t) = \left(\frac{Q_a C' - t_{H^+} \frac{I(1-y_f)}{nF} + D_{H^+} \frac{S_d}{\ell} C''}{Q_2 + D_{H^+} \frac{S_d}{\ell}} + D_{H^+} \frac{S_d}{\ell} t \right) \left[1 - \exp\left(-\frac{Q_2 + D_{H^+} \frac{S_d}{\ell}}{V_a} t\right) \right] + C' \exp\left(-\frac{Q_2 + D_{H^+} \frac{S_d}{\ell}}{V_a} t\right)$

where:
 ρ = specific gravity of the brine at the inlet of the anode
 ρ' = specific gravity of the brine at the outlet of the anode or the inlet of the cathode
 ρ'' = specific gravity of the brine at the outlet of the cathode
 α = number of moles of water removed by Cl_2 stream distillation
 β = number of moles of water removed by H_2 stream

Appendix 2.: Nomenclature

C'	molar concentration (mol m^{-3}) of: ${}^{-j} = \circ$ brine (ions Cl^- and Na^+) supply the anodic compartment, ${}^{-j} = \prime$ acidic solution (H^+ from HCl or H_2SO_4) supply the anodic compartment, ${}^{-j} = \prime\prime$ H^+ flowing across the diaphragm to the cathodic compartment, ${}^{-j} = \prime\prime\prime$ H^+ at the outlet of the cathodic compartment,
C_j	molar concentration (mol m^{-3}) of: ${}^{-j} = 1$ Cl^- flowing across the diaphragm to the cathodic compartment, ${}^{-j} = 2$ Na^+ flowing across the diaphragm to the cathodic compartment, ${}^{-j} = 3$ Cl^- at the outlet of the cathodic compartment, ${}^{-j} = 4$ Na^+ at the outlet of the cathodic compartment, ${}^{-j} = 5$ ions ClO^- at the outlet of the cathodic compartment,
C_{in}	inlet concentration of chloride in the anodic compartment (after mixing of brine and acid),
D	diffusion coefficient ($\text{m}^2 \text{s}^{-1}$),
F	Faraday constant (C mol^{-1}),
F_{in}, F_o	inlet and output molar flux respectively (mol s^{-1}),
I, i	current and current density (A or $A \text{m}^{-2}$),
k	mass transfer coefficient (m s^{-1}),
K	integration constant,
n	exchanged electron number,
Q_j	volumetric flow ($\text{m}^3 \text{s}^{-1}$) of: ${}^{-j} = 1$ acidified brine supply the anodic compartment,

${}^{-j} = 2$	anolyte flowing across the diaphragm to the cathodic compartment,
${}^{-j} = 3$	solution (water) removed by stream distillation (Cl_2),
${}^{-j} = 4$	water removed by the gaseous hydrogen from the cathode,
${}^{-j} = 5$	solution at the outlet of the cathodic compartment,
Q'	acidic solution supply the anodic compartment,
ℓ :	thickness of the ceramic diaphragm,
S_d	geometrical area of the ceramic diaphragm,
S	geometrical area of the electrode used,
$S_{of} Cl_2$	solubility of chlorine,
t	time (s, or h),
t_j	transference number of species j ,
T	temperature ($^{\circ}C$),
u_j	ionic mobility of the ion j ($\text{m}^2 \text{s}^{-1} \cdot V^{-1}$),
V_a and V_c	volume of the anolyte and catholyte respectively (m^3),
V_p	volume of the NaOH trapping solution of the produced gaseous chlorine (9, Fig. 3) (m^3),
X	conversion (%),
y_f	faradic yield (%),
z_j	valence number of the ion j .

Greek letters

α, β	number of moles of water removed respectively by Cl_2 and H_2 stream distillation,
δ	thickness of the diffusion layer (m),
ρ, ρ'	specific gravity of the brine respectively at the inlet and at the outlet of the anode (kg m^{-3}),
ρ''	specific gravity of the brine at the outlet of the cathode (kg m^{-3}),
τ	residence time (s).

Appendix Additional. sub/super scripts

“ in, o, d, \circ , r, m, c, D, acc and lim” are respectively: inlet, outlet, diaphragm, initial, reaction, migration, convection, diffusion, accumulation and limiting.

References

- [1] A.T. Kuhn, C.J. Mortimer, The efficiency of chlorine evolution in diluted brines on ruthenium dioxide electrodes, *J. Appl. Electrochem.* 2 (1972) 283–287.
- [2] Sergio. Trasatti, Progress in the understanding of the mechanism of chlorine evolution at oxide electrodes, *Electrochim. Acta* 32 (3) (1987) 369–382.
- [3] S. Ferro, A. De Battisti, I. Duo, Ch. Comminellis, W. Haenni, A. Perret, Chlorine evolution at highly boron-doped diamond electrodes, *J. Electrochem. Soc.* 147 (7) (2000) 2614–2619.
- [4] Mário H.P. Santana, Luiz A. De Faria, Oxygen and chlorine evolution on $RuO_2 + TiO_2 + CeO_2 + Nb_2O_5$ mixed oxide electrodes, *Electrochim. Acta* 51 (17) (2006) 3578–3585.
- [5] Mário H.P. Santana, Luiz A. De Faria, Oxygen and chlorine evolution on $RuO_2 + TiO_2 + CeO_2 + Nb_2O_5$ mixed oxide electrodes, *Electrochim. Acta* 51 (17) (2006) 3578–3585.
- [6] Didier Devilliers, Henri Groult, Matériaux anodiques pour électrolyseurs, *Can. J. Chem. Eng.* 76(6) 991–999, Article first published online: 27 Mar 2009.
- [7] Shenyng Chen, Yinghan Zheng, Siwen Wang, Xueming Chen, Ti/RuO₂-Sb₂O₅-SnO₂ electrodes for chlorine evolution from seawater, *Chem. Eng. J.* 172 (1) (2011) 47–51.
- [8] V. Panić, A. Dekanski, V.B. Mišković-Stanković, S. Milonjić, B. Nikolić, On the deactivation mechanism of RuO_2 - TiO_2 /Ti anodes prepared by the sol-gel procedure, *J. Electroanal. Chem.* 579 (1) (2005) 67–76.

- [9] R.D. Coteiro, A.R. De Andrade, Electrochemical oxidation of 4-chlorophenol and its by-products using Ti/Ru_{0.3}M_{0.7}O₂ (M= Ti or Sn) anodes: preparation route versus degradation efficiency, *J. Appl. Electrochem.* 37 (2007) 691–698.
- [10] Geoffroy R.P. Malpass, Rodrigo S. Neves, Artur J. Motheo, A comparative study of commercial and laboratory-made Ti/Ru_{0.3}Ti_{0.7}O₂ DSA® electrodes: “in situ” and “ex situ” surface characterisation and organic oxidation activity, *Electrochim. Acta* 52 (3) (2006) 936–944.
- [11] G. Valensi, E. Deltombe, N. de Zoubov et M. Pourbaix, Comportement électrochimique du chlore. Diagramme d'équilibres tension-pH du système Cl-H₂O à 25°C (rapport technique RT.44 du CEBELCOR, février 1957). et Marcel Pourbaix diagramme E/PH.
- [12] Hugh L. McCutchen, Michael R. Tighe, Swimming pool chlorinator system US 4129493 A (1978).
- [13] Joel Grayson, IV, Donald P. Kahle 'Chlorinator', US 4241025 A (1980).
- [14] Rodney L. Glore, Herbert F. Glore, 'Pool chlorinators', US 5034110 A (1991).
- [15] Luke C. Adam, Gilbert Gordon, Direct and sequential potentiometric determination of hypochlorite, chlorite, and chlorate ions when hypochlorite ion is present in large excess, *Anal. Chem.* 67 (3) (1995) 535–540.
- [16] N. Kristajic, V. Nakic, M. Spasojevic, Hypochlorite production II. Direct electrolysis in a cell divided by an anionic membrane, *J. Appl. Electrochem.* 21 (7) (1991) 637–641.